Journal of Engineering Mechanics and Machinery (2025)
Clausius Scientific Press, Canada

DOI: 10.23977/jemm.2025.100117
ISSN 2371-9133 Vol. 10 Num. 1

Numerical simulation of the ground vortex of the Trent700 engine in ground idle: As a reference for the safe maintenance of the engine

Chen Jun

Nanjing University of Aeronautics and Astronautics, Nanjing, Jiangsu, China

Keywords: Ground vortex, Trent700 engine, Wind speed, Wind directon, Numerical simulation

Abstract: The Airbus A330 with Trent 700 engines may form ground vortices during ground maintenance due to the small gap between the air inlet cowl and the ground, which affects engine performance. A three - dimensional model of the engine is established for numerical simulation. The computational domain, mesh, and boundary conditions are set, and the method is verified. Different wind speeds (1 - 9 m/s) and directions are calculated. Results show that under cross - wind, the ground vortex intensity first increases then decreases with wind speed, being stronger at 3 - 4 m/s and moving along the wind. At 4 m/s, the intensity peaks at about 210 ° wind direction, causing severe distortion at the inlet cowl outlet. This research is crucial for engine ground - test maintenance.

1. Introduction

The Airbus A330 is currently one of the most numerous modern large civil transport aircraft in service. To improve the aircraft's fuel efficiency, it is equipped with ultra-high bypass ratio (UHBR) Trent 700 turbofan engines and uses a conventional wing hoist layout. In its routine maintenance work, some aircraft and engine components need to be tested on the ground to verify their technical condition and reliability during replacement or repair. However, the selection and installation characteristics of the A330 aircraft engine result in a small gap between the air inlet cowl and the ground. When operating under static or near-static conditions, the engine can experience lip separation on the windward side of the inlet cowl and form vortex that extend from the ground stagnation point to the inlet cowl, known as ground vortex (Figure 1). These vortex generate considerable hysteresis pressure loss and flow distortion on the fan surface of the engine, affecting engine efficiency and the structural integrity of the fan. In addition, the ground vortex generate forces that draw debris from the ground into the inlet cowl, which can wear down the rotating parts of the engine (Figure 2), clog the turbine blade cooling channels, and reduce the engine's service life; In severe cases, it can injure the fan or compressor blades, causing structural damage[1]. Therefore, consider and validate the impact of ground vortex intake on engine performance and stability as well as safe operation during engine maintenance.

Figure 1 Ground vortex caused by ground idle of Trent700 engine

Figure 2 Erosion of the inlet cone due to FOD

2. Literature Review

In order to explore and solve the problem of ground vortex flow distortion encountered by high bypass ratio engines during near-ground operation, researchers at home and abroad have conducted extensive studies on ground vortex. In terms of generation theory, Klein[2] proposed three necessary conditions for the formation of ground vortex, arguing that the formation of ground vortex requires the presence of a stagnation point on the ground, as well as an upward airflow between the stagnation point and the inlet cowl. He believes that the vortex of the ground vortex come from the shear layer between the fluids. Siervi et al.[3] conducted a simulation experiment in a water tunnel using a simplified and scaled-down model of the intake, and found the effect of velocity magnitude on the formation of ground vortex, and discovered that ground vortex would still occur even if the incoming flow was uncycled. Ma Shenyi[4] discussed the phenomenon of ground vortex and their impact on aircraft and engine safety. He analyzed ground vortex using vortex theory and discussed

the formation and composition of ground vortex, including a central vortex core and an outer free vortex region. He analyzed the distribution of tangential velocity along the radial direction and compared it with theoretical calculations. The accuracy of the vortex theory in analyzing ground vortex was confirmed. Zhao Guangmin[5] analyzed the necessary conditions for the formation of ground vortex and the direction of rotation, and proposed a theoretical flow model of ground vortex. In terms of experimental research, S. Brix[6] conducted experiments using a measurement technique, including a rotating fiber splitting probe, in the engine inlet. Data from these experiments, along with flow measurement and visualization studies, revealed new findings about the structure, location, and intensity of ground vortex. Luis Gustavo Trapp[7]-[8] studied the different compositions and morphologies of ground vortex using a computational fluid dynamics approach and calculated the vortex circulation inside and outside the engine inlet. Ribeiro's[9] study on unsteady analysis of ground vortex absorption using the lattice Boltzmann method, Very Large Vortex Simulation (LBM-VLES), compared the simulation data with the experimental data to capture the dynamic behavior of the vortex and their impact on engine performance. Derek A. Nichols and Bojan Vukasinovic[10] experimentally investigated the control of inlet flow in the engine nacker model under crosswine conditions, explored the evolution of separation patterns caused by cross-flow, and evaluated different fluid-based control strategies. In numerical simulation, Amarnatha S.Potturi et al.[11] discussed computational analysis of the inlet ground vortex experiment using CFD software. Three AIAA-recommended cases were simulated using four different turbulence models (Hellsten's nonlinear model, the achievable k-ε model, Spalart-Allmaras model, and Menter's SST model). Luis Gustavo Trapp and Kelvin Cristofalo de Morais et al. [12] compared the computational fluid dynamics (CFD) results of the ground vortex simulation with the experimental data from the 5th AIAA Symposium on Propulsion Aerodynamics. The study focused on the engine compartment close to the ground, creating vortex between the intake and the ground to simulate the situation before the aircraft took off. Selvanayagam and Aliaga et al. [13] present the study of computational fluid dynamics (CFD) simulation of ground vortex inlet using ANSYS Fluent software. The main objective was to evaluate the ability of ANSYS Fluent software to predict ground vortex effects near the inlet under crosswind conditions.

In this paper, a three-dimensional model of the Airbus A330 equipped with the Trent700 engine, which is widely used in civil aviation operations, was established during the test run of maintenance. The ground vortex field under typical working conditions such as different wind speeds and directions was simulated and analyzed, and the distribution characteristics and variation patterns of the ground vortex field of this type of engine were obtained. This paper presents precautions during ground tests, which can be used as a reference for the safe maintenance of the engine.

3. Model and calculation method

3.1 Computational Model

The three-dimensional digital-model diagram is shown in Figure 3, in which the characteristic size of the intake is H/Di approximately 0.88. In the project modeling process, the structures such as the engine nacelle hanger, engine, landing gear and wing flap aileron section that do not affect the technical results were simplified.

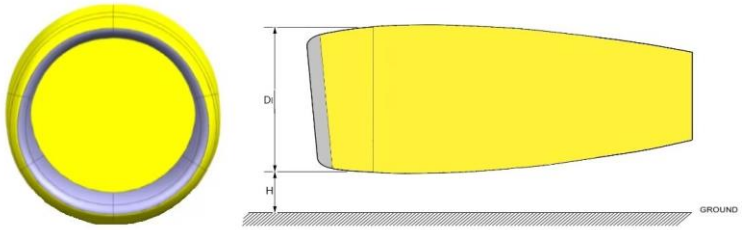

Figure 3 three-dimensional digital model of the Trent700 engine

3.2 Meshing and boundary conditions

Select Dl as the feature size of the inlet cowl, and the model calculation domain size is 30Dl × 30Dl × 15Dl. To better capture ground vortex, the meshes were densized near the wall of the nacelle inlet cowl, in the area below the lip, and on the ground below the inlet cowl, and structured meshes were used for grid independence tests. As shown in Figure 4, when the number of meshes was 4 million, the number of PIV plane loops was relatively small. When the number of meshes increased to 8 million, The ring volume in the PIV plane increased, and the number of meshes was further increased to 10 million, the change in the ring volume was not obvious. Zantopp[14] analyzed the impact of the number of meshes on the calculation results in his article on ground vortex, and the study showed that the generation of ground vortex could be fully observed with 8 million meshes, and this phenomenon could be captured relatively accurately. To sum up, the model mesh selected in this paper is approximately 8 million, and the computational domain and mesh are shown in Figure 5.

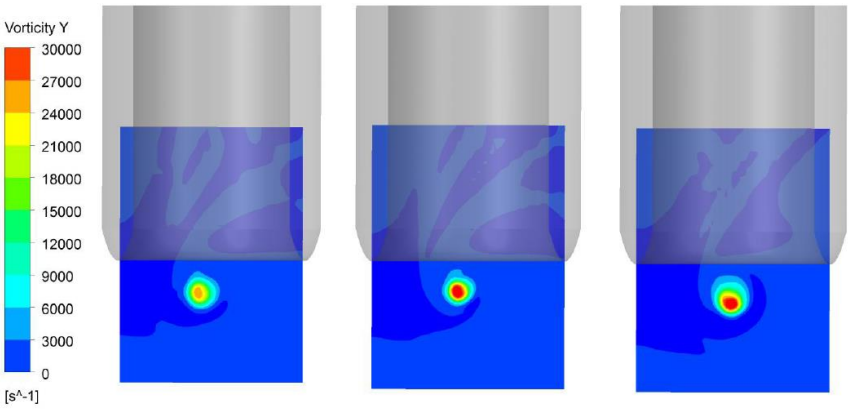

Figure 4 Comparison of vortex cloud maps (the mesh numbers from left to right are: 4M, 8M, 10M)

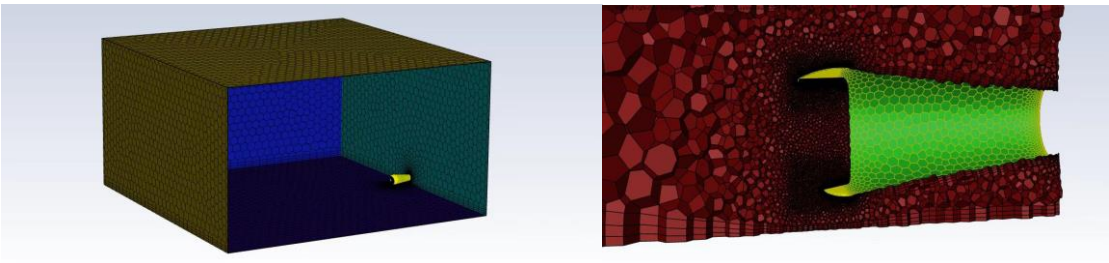

Figure 5 Computational domains and meshes

The boundary conditions are set as shown in Figure 6, and the outer boundaries of the calculation domain are all pressure far-field boundary conditions except for the bottom which is a non-slip wall boundary condition. The inlet pressure outlet boundary condition will be set based on the inlet outlet pressure measurement obtained during the ground maintenance test run of the engine; The rear end face of the nacelle is the velocity inlet boundary condition. Similarly, the velocity value is set based on the velocity value of the airflow at the outlet of the tail nozzle measured in the ground test. The wall of the nacelle is a non-slip wall boundary condition. The CFD commercial software Fluent 2022 was used for the calculation, density-based solver was employed, flux difference splitting was used for the flux, and the control equations were discretized using the second-order windside scheme. The turbulence model was the SST (shear stress transport) k -ω model.

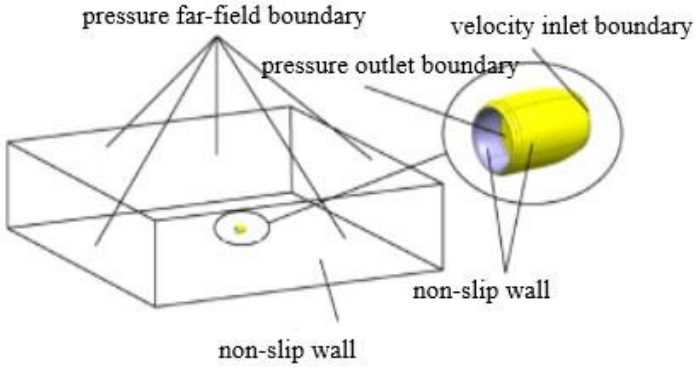

Figure 6 Schematic diagram of boundary condition Settings

3.3 Example verification

In order to verify whether the selected boundary conditions and turbulence model can accurately simulate the structure of the ground vortex intlet vortex system and the flow field distribution, the adopted numerical simulation method is verified first before conducting the simulation. The verification example is the ground vortex test conducted by Murphy et al[15]. in the low-speed wind tunnel at Cranfield University, as shown in Figure 7. The model is a 1/30 scale model, where Dl is the leading edge diameter of the inlet and Di is the inner diameter of the intake. Murphy et al. conducted four ground vortex tests at the height of the inlet cowl from the ground. In this paper, the test points with dimensionless height from the ground h/D_l=0.25 and side winds of 20, 25, and 30 m/s were selected for verification. In the Γ test, Murphy et al. selected the section at a height of

h/Dl=0.083 from the ground as the test flow field measurement section, and the numerical simulation also cut the section at this position for flow field analysis. The comparison between the dimensionless loop quantities of the numerical simulation and the test values is shown in Figure 7, where Vi is the axial velocity at the inlet and V∞ is the relative velocity of the free flow, and is the loop quantity. It can be seen that the numerical simulation is slightly larger than the test measurement, but the trends of the loop quantities of the two are in good agreement. Figure 8 shows the comparison of the ground vortex lines between the numerical simulation and the experimental measurement. It can be seen that the positions of the ground vortex are basically the same, and the vortex distribution is similar. Therefore, the numerical simulation method used in this study can be applied to the calculation of ground vortex.

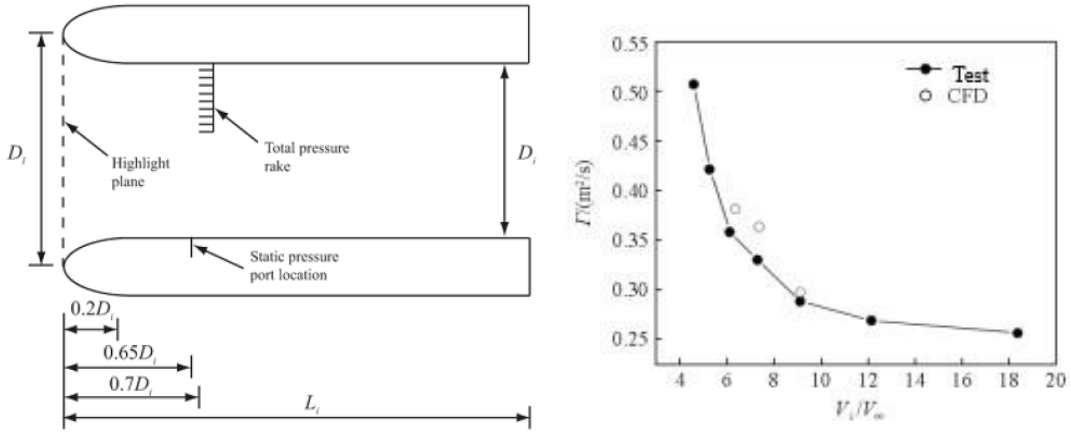

Figure 7 comparison between the dimensionless loop quantities of the CFD and the test value

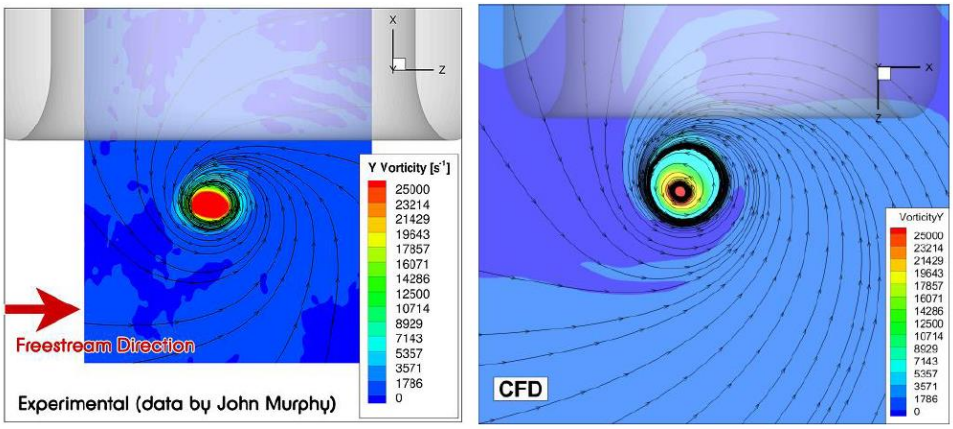

Figure 8 Comparison of cross-sectional flow field structures

4. Data processing methods and computational condition design

4.1 Data processing methods

The intensity and characteristic parameters of ground vortex are mainly cyclic quantities, the cyclic quantity τ of ground vortex, and τ is defined as[16]

$$\Gamma = \oint_l V \cdot \mathrm{d}l = \iint_S (\nabla \times V) \cdot \mathrm{d}S \tag{1}$$

Where V is the velocity vector along the closed curve, l is the closed curve surrounding the ground vortex, and S is the surface enclosed by the closed curve, the dimensionless cyclic quantity Γ * for the above ground vortex is defined as

$$\Gamma^* = \frac{\Gamma}{D_l V_i} \tag{2}$$

Where D_l is the leading edge diameter of the inlet lip and Vi is the axial velocity at the inlet outlet. If there are both positive and negative ground vortex (characterizing positive and negative according to the direction of rotation of the ground vortex), the total loop Γt is calculated as follows

$$\Gamma_t = \left|\Gamma^+\right| + \left|\Gamma^-\right| \tag{3}$$

The pressure difference index Δps represents the static pressure difference between the center of the vortex core and the outside, which characterizes the ability to draw in external objects from the ground vortex. The greater the pressure difference, the greater the intensity of the vortex and the stronger the ability to draw in external objects

$$\Delta p_s = p_{max} - p_{min} \tag{4}$$

Since the suction of ground vortex causes pressure distortion at the engine inlet section, the pressure distortion is characterized by the circumferential total pressure distortion index Δ-σ0, which is defined as follows:

$$\Delta\overline{\sigma_0} = 1 - \frac{\sigma_0}{\sigma_{av}} \tag{5}$$

Where σ0 is the total pressure recovery coefficient in the low-pressure area. σav is the surface average total pressure recovery coefficient, defined as

$$\sigma_{av} = \frac{p^*_{av}}{p^*_0} \tag{6}$$

Where p*a v is the average total pressure at the inlet surface and p*0 is the total pressure of the free flow.

4.2 Calculate the working condition design

According to the theory of ground vortex intake distortion, the generation and distortion intensity of ground vortex are related to factors such as the characteristic size H/Dl of the inlet cowl, external wind speed V∞, wind direction, engine condition, and sliding speed. In the calculation of this paper, the engine test state on the ground (stationary state) and the characteristic size of the inlet cowl are taken as constant values. Five conditions are calculated when the wind level is 1-5 (one condition is selected for each wind level, corresponding to wind speeds of 1, 3, 4, 6, and 9m/s), and the side wind (with a wind direction Angle of 270 °). Based on the above calculation results, it was found that the ground vortex formed when the wind speed was at level 3 were stronger. Then, the wind speed of level 3 was selected as 4 m/s, and the wind direction Angle was selected as 180-360 ° for calculation, with one calculation every 45 °. Seven working conditions were calculated, see figure 9 and Table 1.

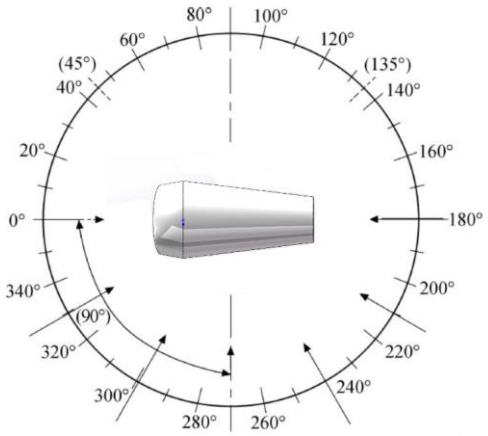

Figure 9 Schematic diagram of wind direction

Table 1 Numerical simulation operating conditions statistics

No.	Wind Angle/ (°)	V∞/ (m/s)
1	270° (crosswind)	1,3,4,6,9
2	180° (tailwind)	4
3	210°	4
4	240°	4
5	270° (tailwind)	4
6	300°	4
7	330°	4
8	360° (headwind)	4

5. Analysis of the calculation results

5.1 Analysis of the influence of wind speed on the ground vortex flow characteristics of Trent700 engine

Take the calculation example when the wind speed V∞ is 4 m/s as a typical working condition to analyze the flow characteristics such as the generation and development of ground vortex distortion. Figure 10 shows the ground vortex flow characteristics when the aircraft is stationary, the wind direction Angle is 270 °, and the wind speed is 4 m/s. From the analysis of the results in the figure, it can be seen that under this condition, due to the strong suction effect of the engine, the air around the lower part of the intake lip converges towards the vertical centerline of the intake lip under the negative pressure formed by the engine suction and forms a stationary point on the ground. At the same time, under the upward suction flow, ground vortex distortion is formed and sucked into the intake. A relatively compact swirl distortion is formed at the engine inlet section.

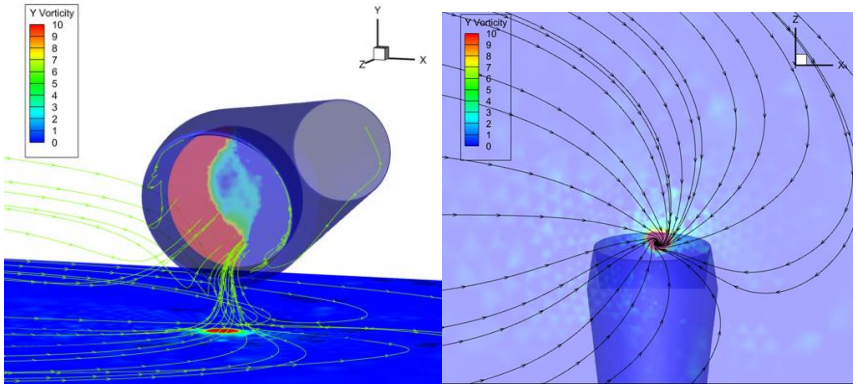

Figure 10 Swirling distortion at the engine inlet section

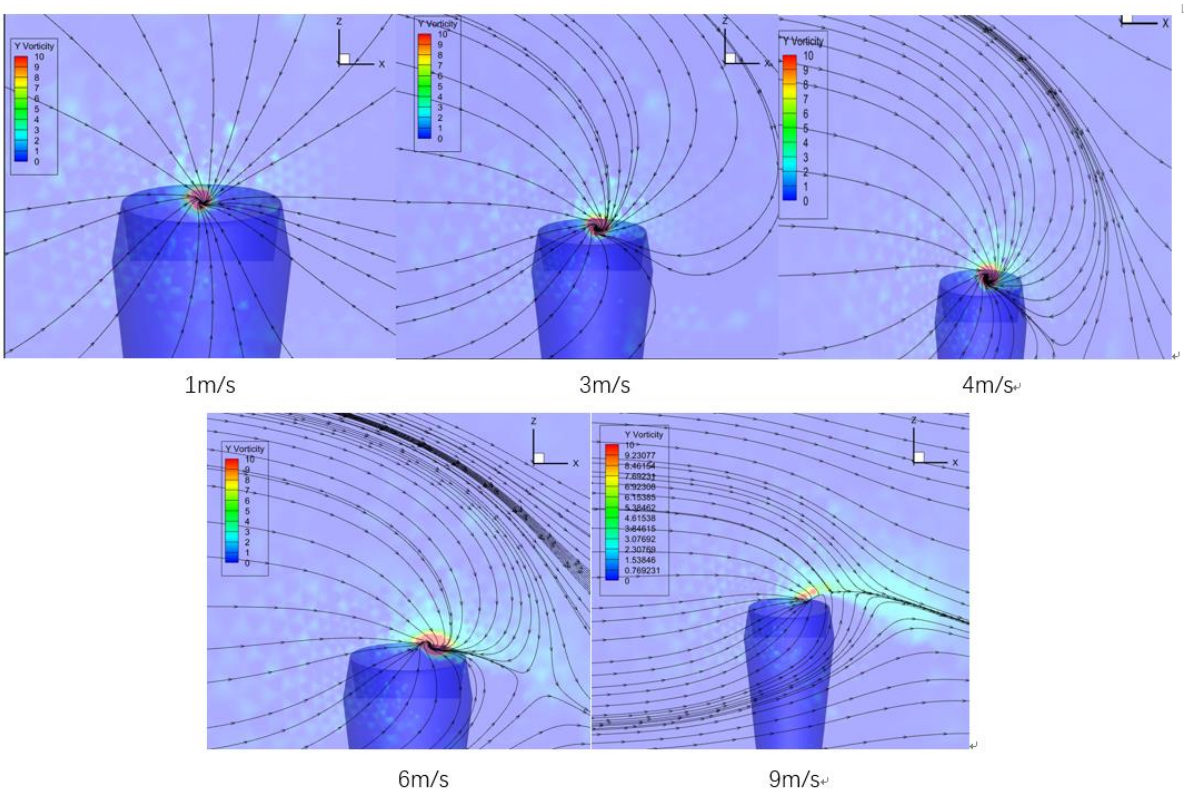

Figure 11 ground vortex flow characteristics under different wind speed conditions

Figure 11 shows the ground vortex flow characteristics under different wind speed conditions when the aircraft is stationary and crosswise. It can be seen from the figure that a single-injection ground vortex is formed under the first-level wind (wind speed 1m/s), and no obvious swirling vortex pattern is seen at the cross-section of the inlet cowl outlet. Under wind speed conditions, that is, within the range of 2 to 6m/s, a distinct main vortex will form in the lip area of the inlet. Ground vortex are stronger when the wind level is 2-3 (3-4 m/s), and the range of swirling distortion formed at the outlet section of the inlet is wider. Additionally, due to the crosswise effect, it can be seen from the figure that the ground vortex move along the wind direction as the wind speed increases. In addition, it can be seen that the effect of the ground vortex intake on the airflow at the engine inlet section is concentrated in the area near the lower wall, and the resulting swirl area is more

compact. When the crosswind speed is 9 m/s, the swirling distortion vortex pattern at the inlet outlet section is small. Figure 12 shows the ground vortex cloud at the inlet outlet under different wind speed conditions. It can be seen that in crosswind conditions, as the incoming wind speed increases, the ground vortex ring volume shows a trend of first increasing and then decreasing. The ground vortex ring volume reaches its maximum when the crosswind wind speed reaches 4 m/s, and then begins to decrease as the wind speed increases. The differential pressure index and the circumferential total pressure distortion at the intake outlet are basically in line with the trend of the ground vortex ring, reaching the maximum when the crosswind speed reaches 4m/s, indicating that the degree of foreign object intake and the pressure distortion caused by the ground vortex are the most severe at this wind speed.

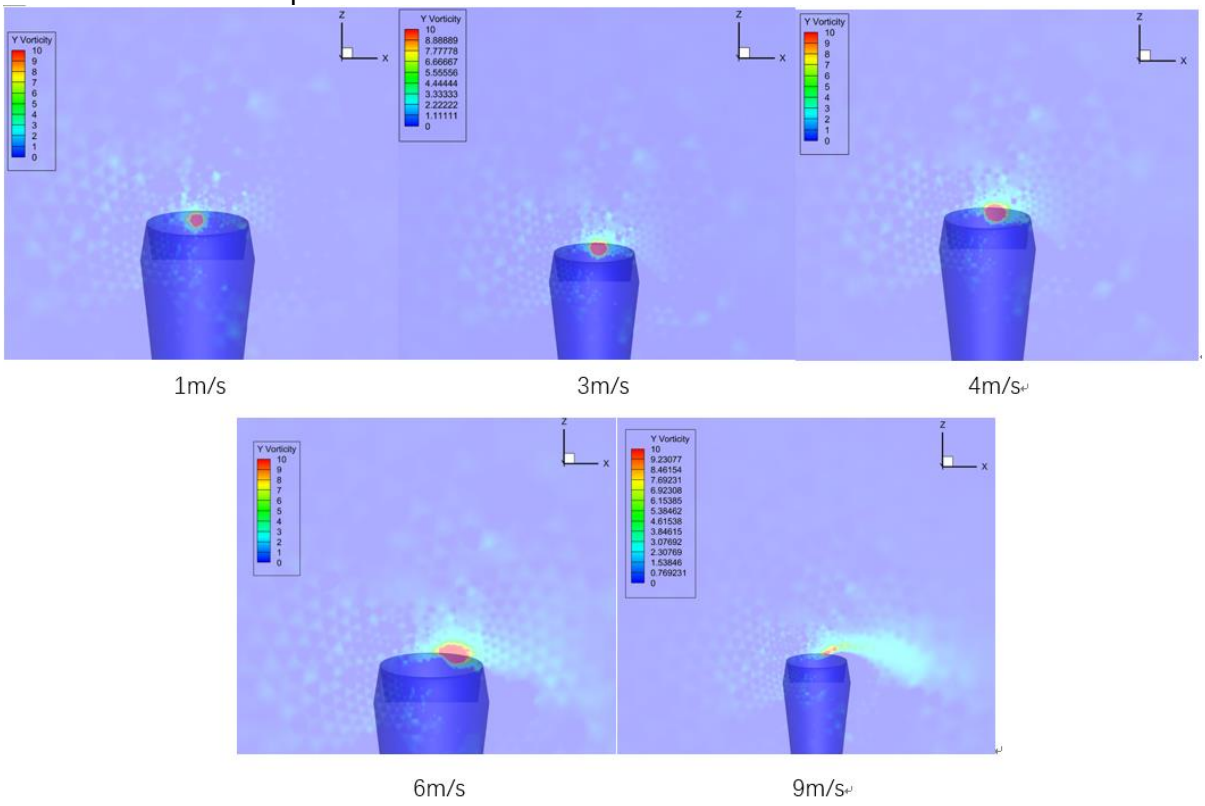

Figure 12 Cloud map of ground vortex under different wind speed conditions

5.2 Analysis of the influence of wind direction on the ground vortex flow characteristics of Trent700 engine

Figure 13 shows the variation of the ground vortex distortion characteristics with the wind direction when the typical wind speed in the stationary state of the aircraft is level 3 (wind speed 4 m/s). At 180 °with the wind and 360 °against the wind respectively, a ground vortex was formed in the lip area of the intake passage. The ground vortex was located slightly to the left directly below the lip of the intake passage short cabin. Due to the effect of this ground vortex distortion, two opposite vortex were formed in the area below the cross-section of the inlet cowl outlet.

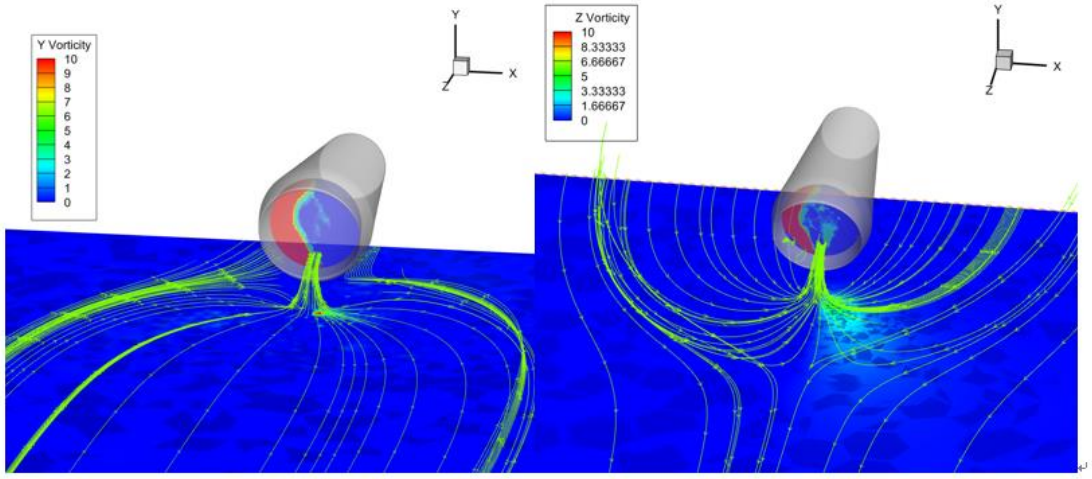

Figure 13 Ground vortex formed by headwind (360 °) and tailwind (180 °) at level 3 winds

In the crosswind condition, that is, within the 210 °-330 ° direction range, a main vortex is also formed in the lip area of the inlet. Due to the crosswind effect and the fact that the crosswind relative to the wind (240 °) is positioned higher than the crosswise relative to the wind (330 °), the positive crosswise (270 °) is positioned relatively centered, see Figure 14. Figure 15 shows the variation cloud of the ground vortex ring volume at the inlet of the intake. Figure 16 shows the flow characteristics of the ground vortex at the inlet.

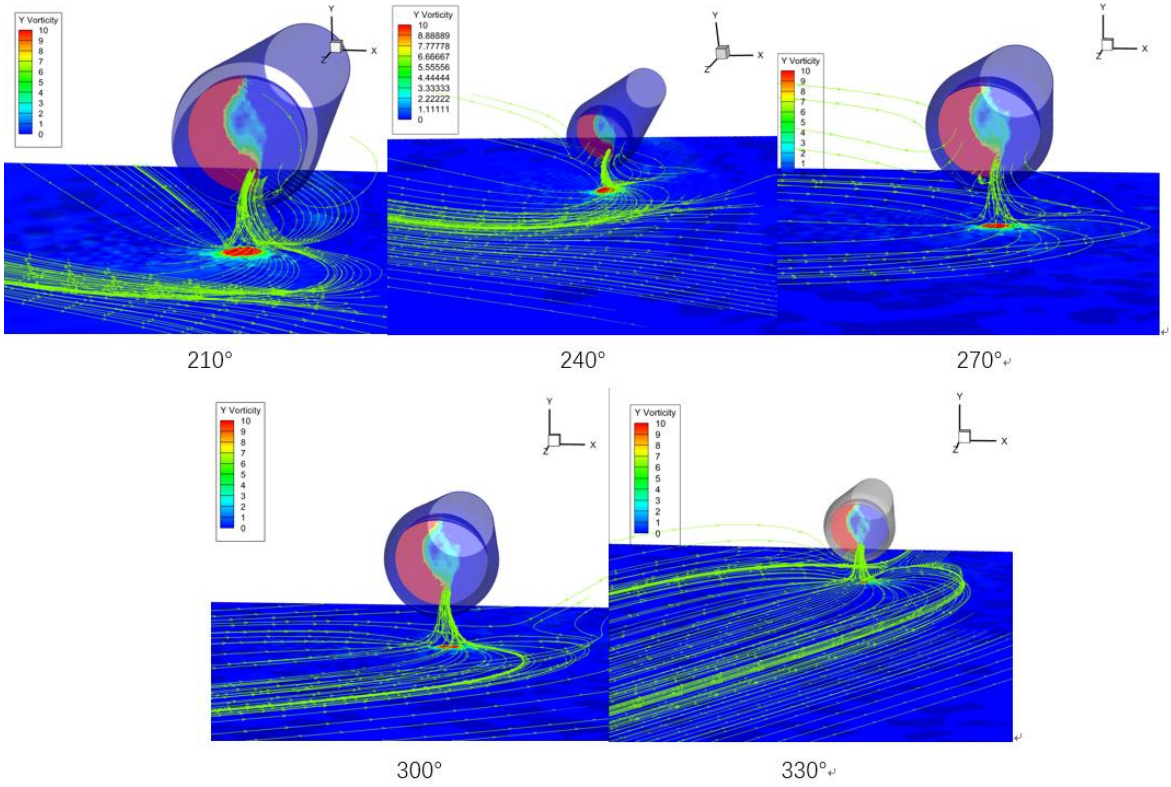

Figure 14 Ground vortex formed by crosswinds at all angles under winds of force 3 (4m/s)

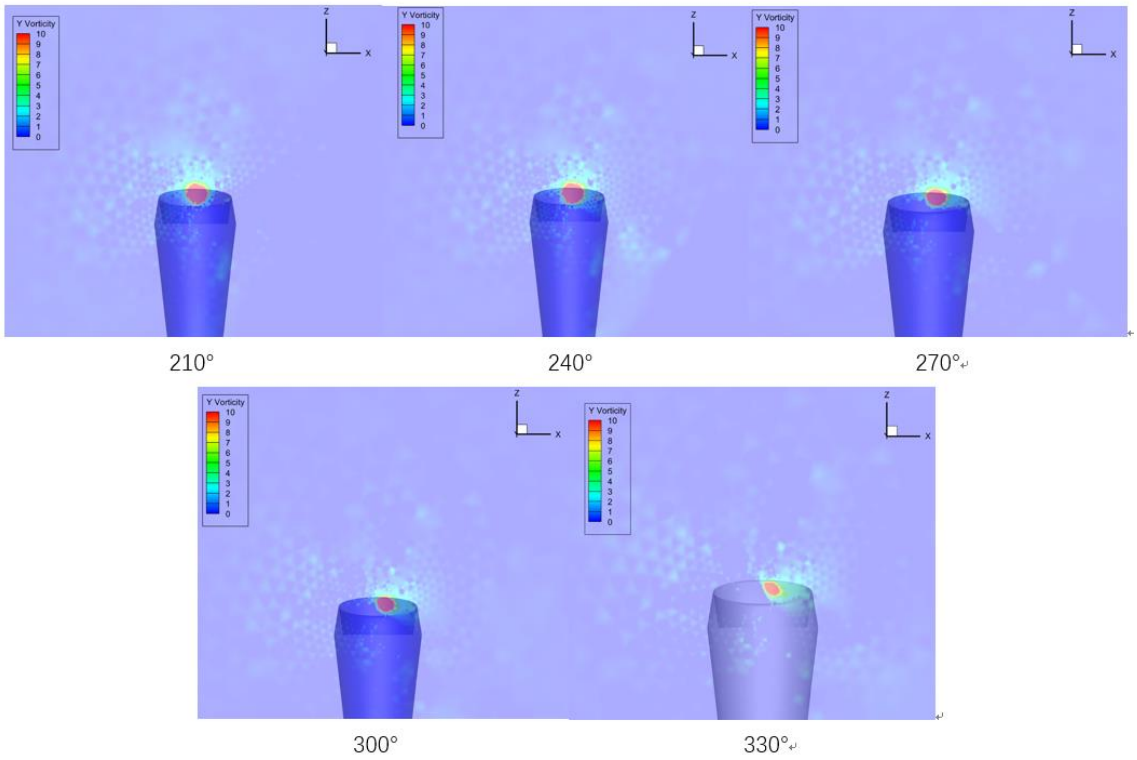

Figure 15 Cloud map of ground vortex formed by crosswinds at all angles under a force 3 wind (4m/s)

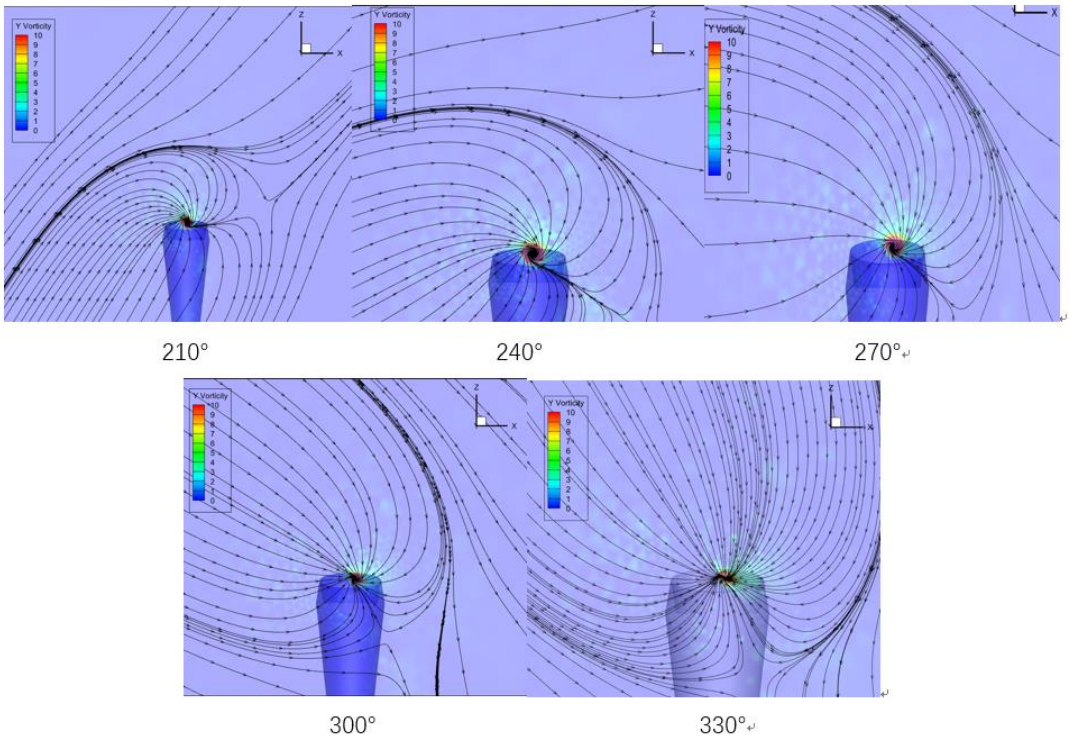

Figure 16 Map of the flow characteristics of ground vortex formed by crosswinds at various angles under force 3 wind (4m/s)

As can be seen from Figures 15 and 16, when the wind speed is the same, as the wind direction increases from 180 ° tailwind to 360 ° tailwind, the ground vortex ring magnitude and the static pressure difference index at the inlet cowl outlet increase first, and the ground vortex ring magnitude and the static pressure difference index are the highest at the wind direction Angle of 210 °. After that, as the wind intensity increases, the ground vortex characteristics weaken, and the ground vortex ring values and static pressure difference index are the smallest at 300 °, and then rise slightly again. By the same token, since the variation of ground vortex directly affects the quality of the flow field at the intake outlet, the circumferential total pressure distortion at the intake outlet is consistent with the trend of the ground vortex ring value. From the above results, it can be known that when the Trent700 engine was tested on the ground, the ground vortex intensity was the greatest within the range of about 210 ° wind direction angle, which caused the strongest distortion at the inlet cowl outlet and the highest suction capacity for foreign objects.

6. Conclusions

Under frontal crosswind conditions, as the wind speed increases, the intensity of the ground vortex in the inlet cowl of the A330 passenger aircraft equipped with Trent700 engines first increases and then decreases until they disappear. The ground vortex formed are stronger when the wind speed is 3-4 m/s, and the ground vortex move along the direction of the wind speed. The ground vortex disappear when the wind speed is above 9m/s. When the wind speed was 4 m/s, during the ground test of this type of aircraft, the intensity of the ground vortex was the greatest around 210 ° wind direction, with the highest suction capacity for foreign objects and the strongest distortion at the inlet cowl outlet.

References

[1] Qu Yuchi, Huo Jianwu. Analysis of Flight Accidents of Large Military and Civilian Aircraft [M]. Xi 'an: China Flight Test and Research Institute, 2009

[2] Klein H J .Vortex inhibitor for aircraft jet engines: US19570686510 [P].US2915262A.DOI:US2915262 A

[3] De Siervi F .Flow visualization study of the inlet vortex phenomenon[J].Massachusetts Institute of Technology, 1981.

[4] Ma Shenyi. Research on ground vortex [J]. Journal of Aeronautica, 1989, 10(5): 4. DOI: CNKI: SUN: HKXB.0.1989-05-013.

[5] Zhao Guangmin, Hu Zong 'an. Fan of the ground vortex generation, and eliminate the [J]. Journal of Beijing university of aeronautics and astronautics, 1986 (4) : 138-142. The DOI: CNKI: SUN: BJHK. 0.1986-04-015.

[6] Brix S , Neuwerth G , Jacob D .The inlet-vortex system of jet engines operating near the ground[C]//Applied Aerodynamics Conference. 2013. DOI: 10.2514/6.2000-3998.

[7] Luis Gustavo Trapp.Crosswind Effects on Engine Inlets: The Inlet Vortex[J].Journal of Aircraft, 2010, 47(2):577-590. DOI:10.2514/1.45743.

[8] Trapp L G, Girardi R D M .Characteristics of Inlet Trailing Vortex[J].American Institute of Aeronautics and Astronautics, 2020 (2). DOI: 10.2514/1. C035565.

[9] Andre F. Ribeiro. "Unsteady Analysis of Ground Vortex Ingestion with LBM-VLES," AIAA 2022-0224. AIAA SCITECH 2022 Forum. January 2022.

[10] Derek A. Nichols, Bojan Vukasinovic, Ari Glezer, Matthew C. DeFore and Bradley Rafferty. "Steady and Unsteady Control of Nacelle Inlet Flow in Crosswind," AIAA 2021-1556. AIAA Scitech 2021 Forum. January 2021

[11] Amarnatha Sarma Potturi, Oshin Peroomian and Paul Batten. "Computational Analysis of an Inlet Ground Vortex Test Case using CFD++," AIAA 2022-1252. AIAA SCITECH 2022 Forum. January 2022

[12] Luis Gustavo Trapp, Kelvin Cristofalo de Morais, Diego F. Abreu and Luiz Tobaldini Neto. "Comparison of CFD Ground Vortex Results with the 5th PAW Intake near the Ground Experiment," AIAA 2022-0223. AIAA SCITECH 2022 Forum. January 2022

[13] Jeyatharsan Selvanayagam, Cristhian Aliaga and John Stokes. "CFD Simulation of Ground Vortex Intake Test

Case using ANSYS FLUENT," AIAA 2022-0222. AIAA SCITECH 2022 Forum. January 2022
[14] Zantopp. Jet engine ground vortex studies[D].Cranfield,UK: Cranfield University,2007.
[15] Murphy J P. Intake groud vortex aerodynamics [D]. Cranfield :Cranfield University,2008.
[16] Tong Binggang, Yin Xieyuan, Zhu Keqin. Vortex motion theory [M]. Hefei: University of Science and Technology of China Press, 2009.